Proceedings of International Structural Engineering and Construction
Holistic Overview of Structural Design and Construction
*Edited by* Vacanas, Y., Danezis, C., Singh, A., and Yazdani, S.

ISSN: 2644-108X

# COMPUTATIONAL ANALYSIS OF HEAT AND MASS TRANSPORT IN CHARACTERISTIC DETAIL OF INTERIOR THERMAL INSULATION SYSTEM

JIŘÍ MADĚRA, JAN KOČÍ, and VÁCLAV KOČÍ

*Dept of Materials Engineering and Chemistry, Faculty of Civil Engineering, Czech Technical University, Prague, Czech Republic*

Computational modeling represents useful tool for the assessment of newly designed or refurbished building materials and structures. Especially, when complex buildings elements need to be assessed from a hygrothermal point of view, the computational modeling is the right approach with desired power and accuracy. In this paper a historical wall element is investigated using two-dimensional simulation in order to study the effect of application of several insulation materials in various scenarios. In total two insulation materials are investigated (mineral wool, wood fiber boards) that are applied in three different scenarios. All simulations are performed under real climatic load. The results of the computational simulations reveal potential weak points in system application and can provide engineers and designers with valuable recommendations and practical information. The best results were obtained for thermal insulation from mineral wool. On the other hand, an improper system application can lead to a significant devaluation of the beneficial effects on the thermal performance of the studied brick element.

*Keywords*: Heat losses, Refurbishment, Wall retrofitting, Historical buildings, Two-dimensional simulations, FEM.

## 1 INTRODUCTION

Interior thermal insulation systems represent one of the possibilities how to retrofit building envelopes. Though they are not as commonly used as the exterior ones, their application is sometimes unavoidable when energy efficiency improvement is the goal (Kim and Yu 2018). Traditional and historical buildings are a typical example in that respect, accounting for 10%-40% of the building stock (Webb 2017).

Since the interior thermal insulation systems show a different interaction with a building envelope than the commonly used insulation, a specific treatment is often required already in the design phase. One must realize that an interior system exposes walls to weather conditions unprotected from the exterior side. Additionally, heat flux from interior is reduced, resulting in a prevention of walls warming. Based on that, several damage patterns may appear such as excessive hygric and temperature straining, frost damage, salt efflorescence or mold growth (Janssens and Hens 2003, Künzel and Zirkelbach 2013). A presence of thermal bridges is another fact that must be struggled with (Abuku *et al.* 2009, Kolatis *et al.* 2013).

Computational modeling represents a useful tool for the assessment of newly designed or refurbished building materials and structures from the hygrothermal point of view. Thanks to well-established and validated mathematical model, precise input parameters and powerful processors, the computational modeling approach is able to provide accurate results in a short period of time without a necessity of a construction being built. Except the time-savings mentioned, this is beneficial also from the economical point view. Additionally, assessment of hygrothermal risk is very complex task requiring rather two-dimensional computation than one-dimensional ones. The one-dimensional calculation may be suitable for example for evaluation of thermal or energy performance. However, when it comes to hygrothermal response of structural elements, the two-dimensional simulations will always provide more reliable view on their performances.

In this paper a critical detail of a historical building element with applied interior thermal insulation systems is assessed using two-dimensional simulation. The objectives of that simulation are to analyze new types of insulation materials applied in several scenarios and reveal potential weak points in system application to provide engineers and designers with valuable recommendations and practical information.

## 2 STUDIED WALL ELEMENT

For the assessment of hygrothermal response a typical building element of historical masonry was chosen. The element contained a brick masonry with the part of a window frame (see Figure 1). This allowed for investigation of several thermal insulation scenarios with a special attention paid to insulation of the jamb. The investigation was done on the horizontal cross-section only with several variants of internal thermal insulation systems (Figure 2).

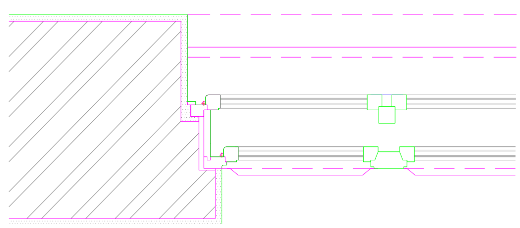

Figure 1. Studied building element – horizontal (left) and vertical (right) cross-section.

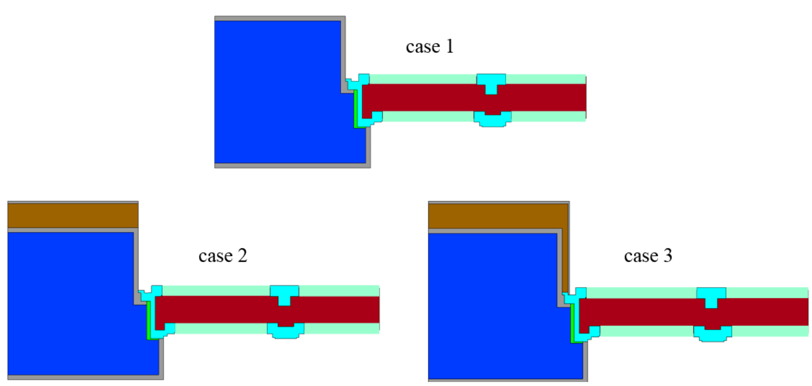


Figure 2. Studied variants of applied thermal insulation.

The first variant (case 1) represents the initial state without thermal insulation in order to provide reference values for the analysis. The second variant (case 2) was based on variant 1 with thermal insulation on the interior surface of the brick wall only. The third variant (case 3) was proceeded from variant 1 with an additional insulation layer connected to the window jamb. As insulation materials, mineral wool and wood fiber boards were investigated. Material properties of the involved materials are summarized in Table 1.

Table 1. Basic parameters of the materials involved in studied wall element.

| | **Ceramic brick** | **Mineral wool** | **Wood fiber board** | **Plaster** |
|---|---|---|---|---|
| Bulk density ($kg \cdot m^{-3}$) | 1831 | 270 | 147 | 1244 |
| Porosity (%) | 27.9 | 93.6 | 90.1 | 49.8 |
| Thermal conductivity ($W \cdot m^{-1} \cdot K^{-1}$) | 0.59 – 1.74 | 0.04 – 0.70 | 0.07 – 0.69 | 0.30 – 0.94 |
| Specific heat capacity ($J \cdot kg^{-1} \cdot K^{-1}$) | 825 – 1254 | 810 – 3850 | 2088 – 3855 | 1054 – 1592 |
| Water vapor diffusion resistance factor (–) | 8.8 – 22.1 | 3.5 – 3.9 | 4.11 – 5.12 | 5.52 – 7.52 |
| Apparent moisture diffusivity ($m^2 \cdot s^{-1}$) | $1.08 \times 10^{-6}$ | $2.51 \times 10^{-10}$ | $5.53 \times 10^{-6}$ | $3.27 \times 10^{-8}$ |

The material parameters of ceramic brick were adopted from Kočí *et al*. (2018a), wood fiber boards from Jerman *et al*. (2019), mineral wool from Jiřičková and Černý (2006) and plaster from Kočí *et al*. (2016).

## 3 COMPUTATIONAL SIMULATION

For the description of heat and moisture transport through porous body a modified Künzel's mathematical model was used (Maděra *et al.* 2017). The model is described by following balance equations in Eq. (1) and (2):

$$c_{eff}\rho_v \frac{\partial T}{\partial t} = div\left(\lambda \operatorname{grad} T\right) + L_v div(\delta_p \operatorname{grad} p_v), \tag{1}$$

$$\left[\rho_w \frac{dw}{dp_v} + \left(n - w\right)\frac{M}{RT}\right]\frac{\partial p_v}{\partial t} = div\left[D_g \operatorname{grad} p_v\right], \tag{2}$$

where $c_{eff}$ ($J \cdot kg^{-1} \cdot K^{-1}$) is the effective specific heat capacity, $\rho_v$ ($kg \cdot m^{-3}$) is the bulk density, $T$ (K) is the absolute temperature, $\lambda$ ($W \cdot m^{-1} \cdot K^{-1}$) is the thermal conductivity, $L_v$ ($J \cdot kg^{-1}$) is the latent heat of evaporation of water, $\delta_p$ (s) is the water vapor diffusion permeability, $p_v$ (Pa) is the partial pressure of water vapor in the porous space, $\rho_w$ ($kg \cdot m^{-3}$) is the density of water, $w$ ($m^3 \cdot m^{-3}$) is the moisture content by volume, $n$ (-) is the porosity of the porous body, $M$ ($kg \cdot mol^{-1}$) is the molar mass of water vapor, $R$ ($J \cdot K^{-1} \cdot mol^{-1}$) is the universal gas constant, and $D_g$ (s) is the global moisture transport function. More information on the modified model can be found in this paper (Kočí *et al.* 2018b). The ice-forming process is described using the smooth effective $c_{eff}$ model, which was implemented into the heat balance equation. The effective specific heat capacity in the temperature range covering freezing or thawing is described in Eq. (3) as:

$$c_{eff} = \begin{cases} c_s & \left(T \le T_1\right) \\ \left[1 - \cos\left(\dfrac{2\pi\left(T - T_1\right)}{T_2 - T_1}\right)\right]^n \left(\dfrac{c_{eff,\max} - c_s}{2^n}\right) + c_s & \left(T_1 < T \le \dfrac{T_1 + T_2}{2}\right) \\ \left[1 - \cos\left(\dfrac{2\pi\left(T_2 - T\right)}{T_2 - T_1}\right)\right]^n \left(\dfrac{c_{eff,\max} - c_l}{2^n}\right) + c_l & \left(\dfrac{T_1 + T_2}{2} < T < T_2\right) \\ c_l & \left(T \ge T_2\right) \end{cases} \tag{3}$$

where $T_1$ and $T_2$ (K) define the temperature range of the phase change $n$ (-) is the transition coefficient, ceff,max is the peak value in transition function, and $c_s$ and $c_l$ ($J \cdot kg^{-1} \cdot K^{-1}$) are the specific heat capacities of frozen and unfrozen sample, respectively. The computational model was implemented into HMS simulation tool, which is based on the general finite element package SIFEL (SImple Finite Elements) (Kruis *et al.* 2010).

Boundary conditions for interior were kept constant at 21 °C and 55 % of relative humidity during the simulation. The exterior conditions were represented by hourly weather data from the Test Reference Year for the location of Olomouc, the Czech Republic.

## 4 RESULTS AND DISCUSSION

In total, three different variants of uninsulated and insulated wall element were studied. Each variant was analyzed with two different materials of thermal insulation systems, which generates 6 computational simulations in total. Case 1 without thermal insulation layer was simulated by FEM using 12 294 nodes and 11 902 elements, with total calculation time of 87 414 seconds. Case 2 with thermal insulation in the interior face of the masonry was simulated using 16 210 nodes, 15 780 elements and took about 153 157 seconds. The last scenario, case 3, with thermal insulation on the entire interior wall surface consisted of 18 131 nodes, 17 627 elements and took approximately 191 030 seconds.

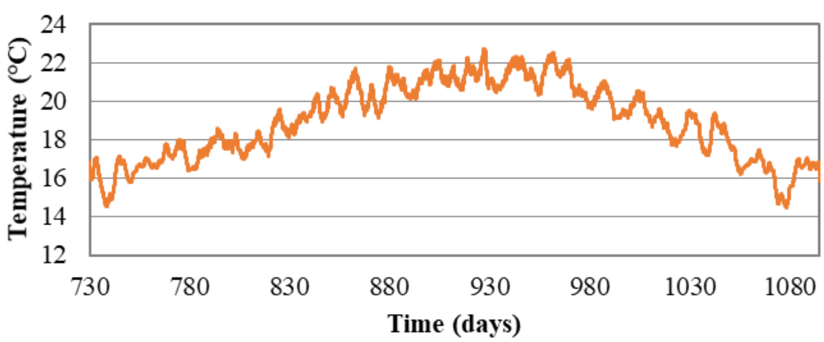


Figure 3. Temperature distribution in the studied point, case 1.

Figure 3 shows the temperature distribution of uninsulated wall element (var1) in the selected most critical point on the surface. The point was located on the interior surface of window jamb right next to the window frame, which exhibited lowest temperature variations during the simulation year. At this point, the risk of possible surface condensation is the highest on the entire surface. Based on the temperature distribution during the year, the most critical (coldest) day was selected (December 15) and for this day the two-dimensional distributions of thermal and relative humidity were generated.

Figure 4 shows the temperature distributions for the cases 2 and 3 for both mineral wool and wood fiber insulations.

It is obvious from Figure 4 that the thermal behavior of case 2 and case 3 is quite different. The thermal insulation on the entire surface of the interior wall (case 3) prevents the interior from heat losses, which supports the cooling of the load-bearing construction from the outside. Therefore, the construction in case 3 is significantly colder than for case 2. This may support water vapor condensation inside the construction. As the temperature and relative humidity of the interior space was kept constant at 21 °C and 55 % of relative humidity, respectively, the dew point in the interior can be found at approximately 11.56 °C, which includes wall surfaces as well. This threshold temperature can be used for a simple analysis to identify potential weak points on the interior surface of the wall.

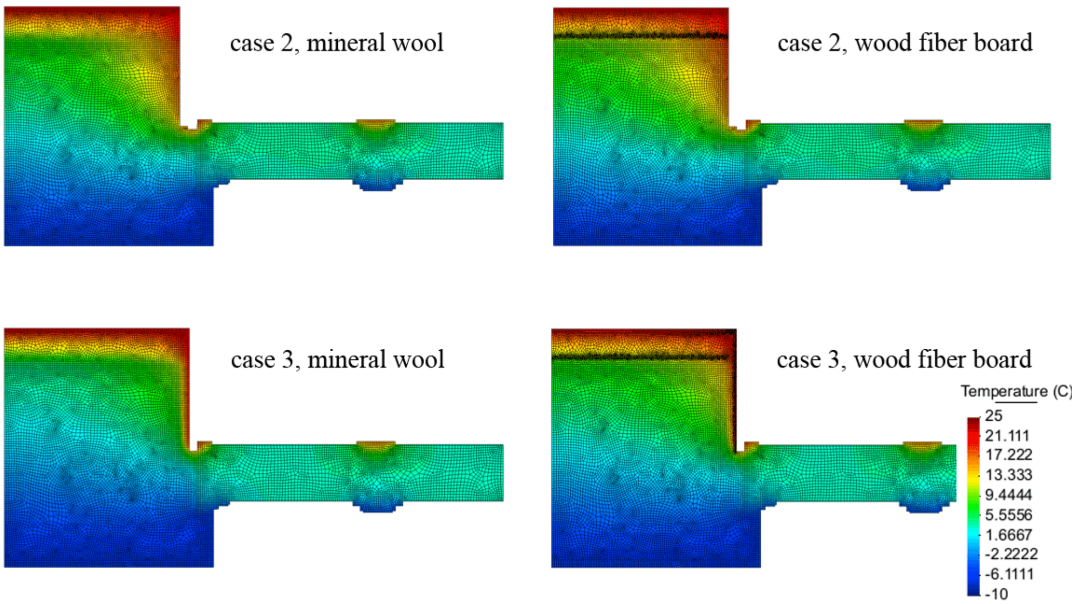


Figure 4. Temperature distribution in the studied wall elements, December 15.

Interesting phenomena can be observed for case 2, when the material of thermal insulation is discussed. The mineral wool exhibits better thermal properties (lower thermal conductivity) than wood fiber board, thus allowing more extensive cooling of the brick body as more heat from the interior is retained in the interior. Since the window jamb is not insulated (and thus creating a thermal bridge), the lower temperature of the brick body with mineral wool is projected in form of colder surface at window jambs. The lowest surface temperature in case of mineral wool was detected as 12.89 °C, while the surface temperature in case of wood fiber board insulation was 13.42 °C. The surface temperature with the insulation on mineral wool was even lower than for case 1 representing the uninsulated wall.

On the other hand, case 3 exhibited higher surface temperatures in comparison with case 2, which is on the safe side regarding the surface condensation. The lowest surface temperatures with mineral wool and wood fiber board were 15.27 °C and 15.07 °C, respectively. Anyway, in all studied cases the surface temperatures did not drop under 11.56 °C.

## 5 CONCLUSIONS

In this paper a series of two-dimensional computational simulations was caried out in order to investigate the hygrothermal response of historical building element made of ceramic brick. The objecitve was also to analyze the response of the element after being thermally insulated by two different insulation materials applied on the interior surface. In total three different scenarios were investigate and several conclusions were drawn. The study supports the fact, that when internal thermal insulation is applied, it must cover entire interior surface to prevent the construction from thermal bridges. If the thermal bridge appears, its effect on the surface temperature depends on the thermal properties of applied insulation. The better insulation means lower surface temperature, which is caused by lower temperature of the load-bearing construction. In this study, the best performance was observed for fully insulated wall with mineral wool, where the surface temperature did not drop under 15.27 °C. The most hazardous conditions were found for partially insulated wall with mineral wool, where the lowest surface temperature was detected at 12.89 °C.

## Acknowledgments

This research has been supported by the Ministry of Culture of the Czech Republic, under project No DG16P02H046.

## References

Abuku, M., Jannsen, H., Roels, S., *Impact of Wind-Driven Rain on Historic Brick Wall Buildings in A Moderately Cold and Humid Climate: Numerical Analyses of Mould Growth Risk, Indoor Climate and Energy Consumption*, Energy and Buildings, 41(1), 101-110, January, 2009.

Janssens, A., and Hens, H., *Interstitial Condensation Due to Air Leakage: A Sensitivity Analysis*, Journal of Thermal Envelope and Building Science, 27, 15-29, July, 2003.

Jerman, M., Palomar, I., Kočí, V., and, Černý, R., *Thermal and Hygric Properties of Biomaterials Suitable for Interior Thermal Insulation Systems in Historical and Traditional Buildings*, Building and Environment, 154, 81-88, May, 2019.

Jiřičková, M., and Černý, R., *Effect of Hydrophilic Admixtures on Moisture and Heat Transport and Storage Parameters of Mineral Wool*, Construction and Building Materials, 20, 425–434, July, 2006.

Kim, J. T., and Yu, C. W. F., *Sustainable Development and Requirements for Energy Efficiency in Buildings - The Korean Perspectives*, Indoor Built Environment, 27(6), 734-751, March, 2018.

Kočí, V., Maděra, J., Jerman, M., Žumár, J., Koňáková, D., Čáchová, M., Vejmelková, E., Reiterman, P., and Černý, R., *Application of Waste Ceramic Dust as A Ready-To-Use Replacement of Cement in Lime-Cement Plasters: An Environmental-Friendly and Energy-Efficient Solution*, Clean Technologies and Environmental Policy, 18(6), 1725–1733, April, 2016.

Kočí, V., Čáchová, M., Koňáková, D., Vejmelková, E., Jerman, M., Keppert, M., Maděra, J., and Černý,R., *Heat and Moisture Transport and Storage Parameters of Bricks Affected by the Environment*, International Journal of Thermophysics, 39(5), 63, March, 2018a.

Kočí, V., Kočí, J., Maděra, J., Pavlik, Z., Gu, X., Zhang, W., and Černý,R., *Thermal and Hygric Assessment of an Inside-Insulated Brick Wall: 2D Critical Experiment and Computational Analysis*, Journal of Building Physics, 41(6), 497-520, January, 2018b.

Kolatis, D. I., Malliotakis, E., Kontogeorgos, D. A., Mandilaris, I., Katsourinis, D. I., and Founti, M. A., *Comparative Assessment of Internal and External Thermal Insulation Systems for Energy Efficient Retrofitting of Residential Buildings*, Energy and Buildings, 64, 123-131, September, 2013.

Kruis, J., Koudelka, T., and Krejčí, T., *Efficient Computer Implementation of Coupled Hydro-Thermo-Mechanical Analysis*, Mathematics and Computers in Simulation, 80, 1578-88, April, 2010.

Künzel, H. M., and Zirkelbach, D., *Advances in Hygrothermal Building Component Simulation: Modelling Moisture Sources Likely to Occur Due to Rainwater Leakage*, Journal of Building Performance Simulation, 6, 346-353, 2013.

Maděra, J., Kočí, J., Kočí, V., and Kruis, J., *Parallel Modeling of Hygrothermal Performance of External Wall Made of Highly Perforated Bricks*, Advances in Engineering Software, 113, 47-53, November, 2017.

Webb, A., *Energy Retrofits in Historic and Traditional Buildings: A Review of Problems and Methods*, Renewable and Sustainable Energy Reviews, 77, 748-759, September, 2017.